

## Nuclear Import and Export Signals Enable Rapid Nucleocytoplasmic Shuttling of the Atypical Protein Kinase C $\lambda^*$

Received for publication, November 15, 2000, and in revised form, December 12, 2000  
Published, JBC Papers in Press, December 13, 2000, DOI 10.1074/jbc.M010356200

Maria Perander<sup>‡</sup>, Geir Bjørkøy, and Terje Johansen<sup>§</sup>

From the Biochemistry Department, Institute of Medical Biology, University of Tromsø, 9037 Tromsø, Norway

The atypical protein kinase C (PKC) isoenzymes,  $\lambda$ - and  $\zeta$ -PKC, play important roles in cellular signaling pathways regulating proliferation, differentiation, and cell survival. By using green fluorescent protein (GFP) fusion proteins, we found that wild-type  $\lambda$ -PKC localized predominantly to the cytoplasm, whereas both a kinase-defective mutant and an activation loop mutant accumulated in the nucleus. We have mapped a functional nuclear localization signal (NLS) to the N-terminal part of the zinc finger domain of  $\lambda$ -PKC. Leptomycin B treatment induced rapid nuclear accumulation of GFP- $\lambda$  as well as endogenous  $\lambda$ -PKC suggesting the existence of a CRM1-dependent nuclear export signal (NES). Consequently, we identified a functional leucine-rich NES in the linker region between the zinc finger and the catalytic domain of  $\lambda$ -PKC. The presence of both the NLS and NES enables a continuous shuttling of  $\lambda$ -PKC between the cytoplasm and nucleus. Our results suggest that the exposure of the NLS in both  $\lambda$ - and  $\zeta$ -PKC is regulated by intramolecular interactions between the N-terminal part, including the pseudosubstrate sequence, and the catalytic domain. Thus, either deletion of the N-terminal region, including the pseudosubstrate sequence, or a point mutation in this sequence leads to nuclear accumulation of  $\lambda$ -PKC. The ability of the two atypical PKC isoforms to enter the nucleus in HeLa cells upon leptomycin B treatment differs substantially. Although  $\lambda$ -PKC is able to enter the nucleus very rapidly,  $\zeta$ -PKC is much less efficiently imported into the nucleus. This difference can be explained by the different relative strengths of the NLS and NES in  $\lambda$ -PKC compared with  $\zeta$ -PKC.

The protein kinase C (PKC)<sup>1</sup> family of lipid-dependent serine/threonine kinases plays pivotal roles in a wide variety of cellular processes (reviewed in Refs. 1–3). Based on sequence homology, domain organization, and biochemical properties, 10 different isoforms are grouped into three classes denoted clas-

sical, novel, and atypical PKCs.  $\zeta$ -PKC and  $\lambda$ -PKC constitute the atypical PKCs (aPKCs). In contrast to the classical and novel PKCs that contain two repeated diacylglycerol (DAG)-binding zinc finger domains within their regulatory domains, the aPKCs have only a single zinc finger domain that is unable to interact with DAG or phorbol esters (4, 5). Consequently, they do not require DAG for their activation. Atypical PKCs have instead been shown to be regulated *in vitro* and *in vivo* by other lipid products such as ceramide (6, 7) and phosphatidylinositol 3,4,5-trisphosphate, a product of phosphatidylinositol 3-kinase (PI 3-kinase) (8–10). Consistently, aPKCs are strongly implicated as downstream effectors of PI 3-kinase (8, 10–14). Recently, evidence has accumulated that imply important roles for aPKCs in processes as diverse as proliferation (15, 16), differentiation (17–19), cell polarity (reviewed in Ref. 20), insulin-mediated up-regulation of general protein synthesis (21), glucose transport (22–24), up-regulation of  $\alpha_2$  integrin gene expression (25), and cell survival (26–30).

Interestingly, in addition to cytoplasmic proteins nuclear proteins also have been reported to act as substrates for aPKCs (31–33). The RNA-binding protein nucleolin is phosphorylated by  $\zeta$ -PKC in response to nerve growth factor (NGF) treatment of PC12 cells (33). Heterogeneous ribonucleoprotein-A1, another RNA-binding protein involved in splicing and mRNA transport, is also a substrate of  $\zeta$ -PKC (31). Both nucleolin and heterogeneous ribonucleoprotein-A1 shuttle between the cytoplasm and the nucleus. The ubiquitously expressed transcription factor Sp1 is able to form a complex with  $\zeta$ -PKC. In fact,  $\zeta$ -PKC phosphorylates Sp1 within the DNA-binding domain and stimulates Sp1-mediated transactivation of the vascular permeability factor/vascular endothelial growth factor promoter (32). Nuclear localization of both  $\zeta$ - and  $\lambda$ -PKC has been demonstrated. NGF stimulation of PC12 cells led to rapid and transient translocation of  $\zeta$ -PKC from the cytoplasm to the nucleus (33–35). In resting HepG2 cells ectopically expressed  $\lambda$ -PKC was found both in the cytoplasm and in the nucleus (8). Upon stimulation with either platelet-derived growth factor or epidermal growth factor, the nuclear pool of  $\lambda$ -PKC translocated in a wortmannin-sensitive manner to the cytoplasm and to more compact structures within the nucleus.

During the last few years, short leucine-rich nuclear export signals (NESs) have been identified within a variety of proteins like human immunodeficiency virus-1 Rev (41), PKI (42), mitogen-activated protein kinase/extracellular signal-regulated kinase kinase (43), mitogen-activated protein kinase-activated protein kinase-2 (MAPKAP-kinase 2) (44), cy-

\* This work was supported by grants from the Norwegian Cancer Society, the Norwegian Research Council, the Aakre Foundation, and the Blix Foundation (to T. J.). The costs of publication of this article were defrayed in part by the payment of page charges. This article must therefore be hereby marked "advertisement" in accordance with 18 U.S.C. Section 1734 solely to indicate this fact.

<sup>‡</sup> Fellow of the Norwegian Cancer Society.

<sup>§</sup> To whom correspondence should be addressed: Dept. of Biochemistry, Institute of Medical Biology, University of Tromsø, 9037 Tromsø, Norway. Tel.: 47-776-44720; Fax: 47-776-45350; E-mail: terje@fagmed.uit.no.

<sup>1</sup> The abbreviations used are: PKC, protein kinase C; aPKC, atypical protein kinase C; GFP, green fluorescent protein; LMB, leptomycin B; NLS, nuclear export signal; NLS, nuclear localization signal; PCR, polymerase chain reaction; DAG, diacylglycerol; PI 3-kinase, phosphatidylinositol 3-kinase; NGF, nerve growth factor; DAPI, 4',6-diamidino-2-phenylindole; HA, hemagglutinin; nt, nucleotide; MAPKAP-kinase 2, mitogen-activated protein kinase-activated protein kinase-2.

TABLE I  
Sequences of oligonucleotides used as PCR primers for plasmid constructions and site-directed mutagenesis

Name	Sequence
APKC.R.5pr	5'-AGTGTGAGAAATTCGCGGACCCAGGAGGACAGC-3'
APKC.3nt	5'-GAATTTCTTAGAGGGGACACATAAAATGCTAA-3'
APKC282W	5'-CGCATTTTATGCAATGTGGGTGTGAAGAAAGAGC-3'
APKC7411A	5'-GGAGACACAAACGCGCTTCTCGGCGACTGCC-3'
APKC7411E	5'-GGAGACACAAACGCGAGGTCTGCGGCACTGCC-3'
APKC.R150/151E	5'-GCCAAACGTTTCAATGAGGAGGCGCACTGTGCGCATC-3'
APKC.F253A/L255A	5'-GCTCTCGACGATCGCATCGCTTCGTCAGTTTAAAG-3'
APKC.A129E	5'-TTACCGGACGAGGAGGACGCGCGTGTGAGAAAGC-3'
gPKC.F252A/L254A	5'-GGGCTCCAAAGACGCTGACGCCATCAAGATCA-3'
gPKC.R281W	5'-AGATTTTACGCAATGTGGGTGTGTGAAGAACGAGC-3'
APKC256.3nt	5'-CCTGCTAGCGCAAGCAAAATCGAAATCTCT-3'
APK.Cent.5pr	5'-GCAGAAATTCGAGTTTCTGCTGAGTTTAA-3'
APKC194.5pr	5'-TGAGTGGAAATTCGCACTCTTTCGCCACCGGAAC-3'
APKC141.5pr	5'-TGTTGGAAATTCGCACACATTTTCAAGCCAAAGT-3'
APKC194.3nt	5'-CAAAGGATCCCGCCGACACATCAATTTGTGACCA-3'
gPKC.5pr	5'-GAGAAATTCCTGCGGACGAGCA-3'
gPKC255.3nt	5'-TGACGCAATCCGAGTCAAAATGCTTGA-3'
gPKC37.5pr	5'-AGGTTGAATTCGCAAAATTCATGCGC-3'
gPKC88.3nt	5'-CCCGGATTCGCAAGCCGACACAGAGAAC-3'
gPKC155.3nt	5'-CTGGGATTCGCAATTCGCGAGAGGCTAG-3'
mgPKC132.5pr	5'-AGCGAAATTCGCACTCTTCCAGGCAAA-3'
mgPKC182.3nt	5'-GAATGGAATCCGCTCTCGCAGGTGAC-3'
gPKC.3nt	5'-ATGTTCTAGACACGAGCTCTCTGACGCA-3'
gcat.5pr	5'-ACTTGAATTCATGAGAGTCTATGCGGG-3'
g130.5pr	5'-GAGCGAAATTCGCACTCTTCCAGGCA-3'
APKC163.5pr	5'-GAATGAATTCCTCTGACAGACAGATACAA-3'
gPKC182.3nt	5'-GAATCGGATCCCTCTGACAGTTCACGGGGA-3'

clin B (45), and phospholipase C- $\delta$ 1 (46). NES-dependent nuclear export is inhibited by leptomycin B that interferes with the binding of NES to CRM1/exportin 1 (47–51).

Here we have studied the subcellular localization of  $\lambda$ - and gPKC in living cells using green fluorescent protein (GFP) fusion proteins. We find that a kinase-defective mutant of APKC accumulates in the cell nucleus, whereas the wild-type kinase is mainly cytosolic. Inhibition of CRM1-dependent nuclear export using leptomycin B leads to rapid nuclear accumulation of both GFP- $\lambda$  and endogenous APKC. By deletion studies and site-directed mutagenesis, we identified both a functional NLS and an NES in APKC. These signals endow APKC with the ability to shuttle continuously between the cytoplasm and the nucleus. Our results are compatible with the notion that the exposure of the NLS in both APKC and gPKC may be regulated by intramolecular interactions between the N-terminal region and the catalytic domain of the kinases. Also, we find that gPKC is much less efficiently imported into the nucleus than APKC in HeLa cells upon blockade of nuclear export by leptomycin B treatment. This is most likely due to differences in the relative strengths of the NES and NLS in the two atypical PKCs.

#### MATERIALS AND METHODS

**Cell Cultures.**—HeLa cells (ATCC CCL2) were grown in Eagle's minimum essential medium supplemented with 10% fetal calf serum, non-essential amino acids, 2 mM L-glutamine, penicillin (100 units/ml), and streptomycin (100  $\mu$ g/ml) (Life Technologies, Inc.). HEK293 cells were maintained in Dulbecco's modified Eagle's medium supplemented with 10% fetal calf serum, and the antibiotics described above. Subconfluent HeLa and HEK293 cells were transfected using the calcium-phosphate coprecipitation method. For the nuclear export experiments, leptomycin B, kindly provided by Dr. M. Yoshida, Tokyo, was added to the medium to a final concentration of 2  $\mu$ g/ml.

**Plasmid Constructions and Site-directed Mutagenesis.**—The murine APKC cDNA was amplified from a mouse brain cDNA library (Marathon Ready, CLONTECH) by PCR using ExTaq polymerase (Takara Biomedicals). The PCR product was made blunt and subcloned into the *Sma*I site of pUC18. Inspection of the cDNA sequences show that both the murine APKC and the human APKC cDNAs actually contain an in frame ATG codon nine codons upstream of the proposed start codon (5, 52). The *Xenopus* APKC also contains this start codon eight amino acids upstream of the second ATG codon. Since this is the first in frame ATG

and the amino acid sequence of this N-terminal extension also are conserved between the species, we suggest that this most 5' ATG is the start codon of  $\lambda$ PKC. Consequently, the numbering system used in this paper is based on this. To generate pHA- $\lambda$ , pUC18-APKC was digested with *Eco*RI and *Xba*I, and the fragment containing the coding region for full-length APKC (amino acids 1–595 in our numbering system) was inserted into the corresponding sites of pCDNA3- $\lambda$ . pCDNA3- $\lambda$  was a kind gift from Dr. Jorge Moscat and contains an influenza hemagglutinin (HA) epitope tag inserted into the *Hind*III-*Eco*RI sites of pCDNA3 (Invitrogen). pGFP- $\lambda$  was made from pHA- $\lambda$  by inserting the *Eco*RI-*Xba*I (blunted) fragment encoding  $\lambda$ PKC into the *Eco*RI-*Sma*I sites of pEGFP-C1 vector (CLONTECH). pGFP- $\lambda$  was made from pHA- $\lambda$  (kindly provided by Dr. Jorge Moscat) by inserting an *Eco*RI-*Xba*I (blunted) fragment encoding rat gPKC into the *Eco*RI-*Sma*I sites of pEGFP-C1. The expression plasmids for HA-AK282W, GFP-AK282W, GFP-AT411A, GFP-AT411E, GFP-AK282W-R150E/R151E, GFP-A141-162/R150E/R151E, GFP-AF253A/L255A, GFP-AA129E, GFP- $\lambda$ K281W, and GFP- $\lambda$ F252A/L254A were made by site-directed mutagenesis according to the instruction manual for the Quick-Change Site-directed Mutagenesis Kit (Stratagene) using the APKC282W, APKC7411A, APKC7411E, APKC.R150E/R151E, APKC.F253A/L255A, APKC.A129E, gPKC281W, and gPKC.F252A/L254A mutagenesis primers (Table I). The GFP- $\lambda$  and GFP-g deletion mutants were made using the following strategy. Different parts of the  $\lambda$ - or gPKC cDNAs were amplified by PCR using primers that contained recognition sequences for specific restriction enzymes. The PCR products were purified and digested with restriction enzymes and inserted into the corresponding sites of pEGFP-C1. All constructs were verified by sequencing. All GFP- $\lambda$ -g constructs are named according to the included parts of either APKC or gPKC with the amino acid positions shown in parentheses. To study the localization of the regulatory domain of APKC, two different constructs were made encoding fusion proteins where GFP was either fused to the N-terminal end or the C-terminal end. pUC18-regA was generated by PCR using pUC18-APKC as template and the APKC.R.5pr and  $\lambda$ 256.3nt primers (Table I). The PCR product was made blunt and subcloned into the *Sma*I site of pUC18. pUC18-regA was digested with *Nhe*I (blunted) and *Eco*RI, and the regA fragment was inserted into the *Apa*I (blunted) and *Eco*RI sites of pEGFP-N1 (CLONTECH). To make pGFP- $\lambda$ 1–256, regA-GFP was cut with *Eco*RI and *Bam*HI, and the regA fragment was cloned into the corresponding sites of pEGFP-C1. pGFP- $\lambda$ 256–595 was made from a PCR product generated by using pUC18-APKC as template and the primers APKC.Cent.5pr and APKC.3nt. The PCR product was cut with *Xba*I (blunted) and *Eco*RI and inserted into *Sma*I-*Eco*RI digested pEGFP-C1. pGFP- $\lambda$ 1–139 was constructed by inserting an *Eco*RI-*Msc*I fragment from pGFP- $\lambda$ 1–256 into the *Eco*RI-*Sma*I sites of pEGFP-C1. pGFP- $\lambda$ 141–595 was made by PCR using the

APKC141.5pr and the  $\Delta$ PKC.3nt primers. The product was cut with *XbaI* (blunted) and *EcoRI* and cloned into the *EcoRI-SmaI* sites of pEGFP-C1. pGFP- $\Delta$ (194–256) was constructed from a PCR product amplified using the  $\Delta$ 194.5pr and  $\Delta$ 256.3nt primers, digested with *EcoRI* and *NheI* (blunted), and inserted into the *EcoRI-SmaI* sites of pEGFP-C1. To make pGFP- $\Delta$ (141–194), the  $\Delta$ 141.5pr and  $\Delta$ 194.3nt primers were used, and the PCR product was cut with *EcoRI* and *BamHI* and inserted into the corresponding sites of pEGFP-C1. Exactly the same strategy was used to make pGFP- $\Delta$ (1–194) and pGFP- $\Delta$ (163–194) using the primers  $\Delta$ PKC.5pr and  $\Delta$ PKC194.3nt for pGFP- $\Delta$ (1–194) and  $\Delta$ PKC163.5pr and  $\Delta$ PKC194.3nt for pGFP- $\Delta$ (163–194) (Table 1). pGFP- $\Delta$ (11–163) was made from pGFP- $\Delta$ (141–194) by inserting an *EcoRI-EcoRI* (blunted) fragment into *EcoRI-SmaI*-digested pEGFP-C1. To make pGFP- $\Delta$ (132–182) a cDNA fragment encoding the zinc finger domain of PKC was amplified from mouse brain cDNA library using the  $\Delta$ PKC132.5pr and  $\Delta$ PKC182.3nt primers (Table 1). The PCR product was cut with *BamHI* and *EcoRI* before being inserted into the corresponding sites of pEGFP-C1. To make pGFP- $\Delta$ (37–88) and pGFP- $\Delta$ (37–155), containing one or both of the zinc finger domains from murine  $\Delta$ PKC fused to GFP, the same strategy as for construction of pGFP- $\Delta$ (132–182) was used except that the  $\Delta$ PKC.37.5pr and  $\Delta$ PKC.88.3nt primers were used for pGFP- $\Delta$ (37–88) and the  $\Delta$ PKC.37.5pr and  $\Delta$ PKC155.3nt primers were used for pGFP- $\Delta$ (37–155). pGFP- $\Delta$ (255–592) and pGFP- $\Delta$ (130–592) were made from PCR products amplified using pHA- $\Delta$ PKC as template and the *cat.5pr* and  $\Delta$ PKC.3nt primers for pGFP- $\Delta$ (255–592) and primers  $\Delta$ 130.5pr and  $\Delta$ PKC.3nt for pGFP- $\Delta$ (130–592). The PCR products were blunted, cut with *EcoRI*, and cloned into the *EcoRI-SmaI* sites of pEGFP-C1. pGFP- $\Delta$ (1–255) was made from a PCR product generated using the  $\Delta$ PKC.5pr and  $\Delta$ PKC255.3nt primers that was cut with *EcoRI* and *BamHI* and inserted into the corresponding sites within pEGFP-C1. pGFP- $\Delta$ (1–182) and pGFP- $\Delta$ (130–255) were generated following exactly the same strategy as for pGFP- $\Delta$ (1–255) using the  $\Delta$ PKC.5pr and  $\Delta$ PKC182.3nt primers for pGFP- $\Delta$ (1–182) and the primers  $\Delta$ PKC130.5pr and  $\Delta$ PKC255.3nt for pGFP- $\Delta$ (130–255).

**Subcellular Localization Assays and Immunocytochemistry.**—For the subcellular localization studies of the different GFP fusion proteins, HeLa cells were seeded in 6-well dishes at a density of  $5 \times 10^5$  cells per well 24 h before transfection. The cells were transfected with 1  $\mu$ g of expression vectors for the different GFP fusions. The subcellular localizations of the GFP fusion proteins in living cells were visualized by fluorescence microscopy using a Leitz DMIRB invert microscope equipped for fluorescence and with a Leica DMO digital camera. For DAPI staining the cells were fixed and permeabilized in 4% paraformaldehyde, 0.01% Triton X-100 for 10 min at 4°C, and the DNA was stained with 1  $\mu$ g/ml DAPI (Sigma) for 5 min at room temperature. HA- $\lambda$  and HA- $\Delta$ K282W were detected using a monoclonal anti-HA antibody (12CA5, Roche Molecular Biochemicals). Subconfluent HEK293 cells in 24-well culture dishes were cotransfected with 0.4  $\mu$ g of the different GFP- $\Delta$ N- $\lambda$ -expressing plasmids and 0.4  $\mu$ g of vectors expressing either HA- $\lambda$  or HA- $\Delta$ K282W. Twenty four h later the cells were fixed by adding freshly made paraformaldehyde directly to medium to a final concentration of 4%. The cells were permeabilized for 10 min on ice using methanol pre-chilled at -20°C. The aldehyde groups were quenched by incubating the cells with 10 mM glycine, pH 8.5, for 5 min at room temperature. The fixed cells were incubated with 3% pre-immune goat serum in phosphate-buffered saline for 1 h at room temperature before incubation with the anti-HA antibody diluted 1:500 in blocking solution for 1 h at room temperature or overnight at 4°C. The immunostaining was developed using an Alexa 568-conjugated goat anti-mouse IgG secondary antibody (Molecular Probes) diluted 1:500 in blocking solution. Endogenous  $\Delta$ PKC in HeLa cells was detected by staining with an anti-APKC antibody (clone 41, Transduction Laboratories) at a dilution of 1:200.

**Preparation of Cytosolic/Nuclear Extracts and Immune Complex Kinase Assays.**—The activities of the different GFP- $\Delta$ N- $\lambda$  mutants and HA- $\Delta$ N- $\lambda$  were measured in total cellular extracts by immune complex kinase assays using histone H1 as substrate. Subconfluent cultures of HeLa cells in 100-mm diameter Petri dishes were transfected with 10  $\mu$ g of vectors expressing the different GFP- $\Delta$ N- $\lambda$  mutants or HA- $\Delta$ N- $\lambda$ . The cells were harvested by trypsinization 24 h post-transfection, and nuclear extracts were prepared as described (53). All buffers contained 1 tablet per 10 ml of Complete Mini, EDTA-free protease inhibitor mixture (Roche Molecular Biochemicals), 1 mM sodium vanadate, and 10 mM  $\beta$ -glycerophosphate. Following isolation of the nuclei by centrifugation, the supernatant containing the cytosolic extract was removed. Finally, the cytosolic and nuclear extracts were mixed to give total cellular extracts. Approximately equal amounts of the different GFP- or HA-

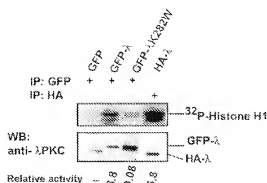
tagged proteins were immunoprecipitated from total cell extracts as follows. Total cellular extracts from 100-mm culture dishes were pre-incubated with unsaturated 50% gel-slurry solution of protein A-Sepharose CL-4B beads (Amersham Pharmacia Biotech) for 20 min at 4°C and then incubated for 2 h at 4°C with either 1  $\mu$ g of anti-HA antibody (12CA5, Roche Molecular Biochemicals) or 2  $\mu$ g of polyclonal anti-GFP antibody (Molecular Probes) in a total volume of 400  $\mu$ l in HA lysis buffer (50 mM Tris-HCl, pH 7.5, 150 mM NaCl, 2 mM EDTA, 1 mM EGTA, 1% Triton X-100). Fifteen  $\mu$ l of bovine serum albumin-saturated 50% gel-slurry was added to the samples before continuing the incubation for 1 h at 4°C. The samples were washed five times in HA lysis buffer and once in  $\Delta$ N-kinase buffer (35 mM Tris-HCl, pH 7.5, 10 mM  $\text{MgCl}_2$ , 0.5 mM EGTA, 0.1 mM  $\text{CaCl}_2$ ). The complexes were resuspended in 15  $\mu$ l of kinase buffer containing 3  $\mu$ g of histone H1 (Calbiochem), 60  $\mu$ M ATP, and 2  $\mu$ Ci of [ $\gamma$ - $^{32}$ P]ATP and incubated at 30°C for 20 min. The kinase reactions were terminated by adding 3.8  $\mu$ l of 5% SDS-polyacrylamide gel electrophoresis gel load buffer, and the samples were boiled immediately for 5 min. The samples were run on a 10% polyacrylamide gel and electrotransferred to a nitrocellulose membrane (Hybond ECL, Amersham Pharmacia Biotech). The phosphorylated proteins were detected and quantitated using a PhosphorImager (Molecular Dynamics). The amount of immunoprecipitated GFP- $\Delta$ N- $\lambda$  and HA- $\lambda$  was determined by probing the membrane with the specific anti-APKC antibody or an anti- $\Delta$ PKC antibody (Upstate Biotechnology) that recognizes both PKC and  $\Delta$ PKC. The chemiluminescence signals from the blots were detected using a LumiImager F1 (Roche Molecular Biochemicals) and quantitated as Boehringer light units using the LumiAnalyst 3.0 software. The relative activities of GFP- $\lambda$  and HA- $\lambda$  were determined as PhosphorImager units of phosphorylated substrate divided on the Boehringer light units representing the amount of kinase used.

**Western Blot Analyses.**—HeLa cells were seeded at  $4 \times 10^6$  per 100-mm dish the day before transfection. The cells were transfected with 10  $\mu$ g of the different GFP- $\Delta$ N- $\lambda$ -expression vectors. Twenty four h post-transfection the cells were scraped directly in 100  $\mu$ l of 2 $\times$  SDS-polyacrylamide gel electrophoresis gel load buffer, boiled for 5 min, and sonicated briefly. The samples were run on 10% SDS-polyacrylamide gels and blotted onto Hybond nitrocellulose membranes. The membranes were blocked in 5% nonfat dry milk in TBST (10 mM Tris-HCl, pH 8.0, 150 mM NaCl, 0.1% Tween 20) for 1 h at room temperature and then incubated with the primary antibody diluted in TBST for 1 h at room temperature or overnight at 4°C. The following primary antibodies were used: anti-GFP, polyclonal (diluted 1:2000, CLONTECH), anti-APKC (0.1  $\mu$ g/ml, clone 41, Transduction Laboratories), anti- $\Delta$ PKC (0.5  $\mu$ g/ml, Upstate Biotechnology, Inc.), and anti-HA (1  $\mu$ g/ml, 12CA5, Roche Molecular Biochemicals). The membranes were washed 6 times in TBST and incubated with horseradish peroxidase-conjugated anti-rabbit IgG or anti-mouse IgG secondary antibodies (0.2  $\mu$ g/ml, Transduction Laboratories) for 1 h at room temperature. The washing step described above was repeated, and the membranes were developed using the ECL system following the instructions of the manufacturer (Amersham Pharmacia Biotech).

## RESULTS

**Different Subcellular Localization of Wild-type  $\Delta$ PKC and Two Mutants with Single Mutations in the Catalytic Domain.**—Vectors for expression of murine  $\Delta$ PKC with either an HA epitope tag or enhanced green fluorescent protein (GFP) fused to its N terminus were constructed. The expressed proteins were denoted HA- $\lambda$  and GFP- $\lambda$ , respectively. A point mutation was introduced into the ATP-binding site to generate a kinase-defective mutant of  $\Delta$ PKC,  $\Delta$ K282W. To test if the relatively large GFP moiety affected the kinase activity of  $\Delta$ PKC, immune complex kinase assays were performed to compare the ability of HA- $\lambda$  and GFP- $\lambda$  to phosphorylate histone H1. As shown in Fig. 1, HA- $\lambda$  and GFP- $\lambda$  immunoprecipitated from transiently transfected HeLa cells showed similar activities with GFP- $\lambda$  even being a bit more active than HA- $\lambda$ . The GFP fusion to the ATP-binding site mutant (GFP- $\Delta$ K282W) showed no activity as expected. This strongly suggests that the fusion of GFP to the N-terminal of  $\Delta$ PKC has no significant effect on kinase activity.

To determine the subcellular localization of  $\Delta$ PKC in living cells, HEK293 and HeLa cells transiently transfected with vectors expressing either GFP- $\lambda$ , GFP- $\Delta$ K282W, or GFP alone were analyzed by fluorescence microscopy. GFP- $\lambda$  was mainly



**Fig. 1. The kinase activity of  $\Delta$ PKC is not affected by the GFP fusion partner.** Subconfluent HeLa cells in 100-mm dishes were transfected with 10  $\mu$ g of either pEGFP-C1 vector or expression constructs for GFP- $\lambda$ , GFP- $\Delta$ K282W, or HA- $\Delta$ . Twenty-four h after transfection, whole cell extracts were made by mixing nuclear and cytosolic extracts as described under "Materials and Methods." GFP, GFP- $\lambda$ , GFP- $\Delta$ K282W, or HA- $\Delta$  were immunoprecipitated (IP) using an anti-GFP antibody or an anti-HA antibody, and their kinase activities were determined using histone H1 as substrate. Protein loading was determined by immunoblotting (WB) with an antibody against  $\lambda$ PKC. The relative activities represent the amount of substrate phosphorylated and quantitated using a PhosphorImager divided on the amount of kinase protein used in the assays quantitated by means of a Luminager.

localized to the cytoplasm in both cell lines although a fraction of the protein was detected in the nucleus (Fig. 2A). Surprisingly, the GFP- $\Delta$ K282W mutant was localized to the cell nucleus in both cell types. The GFP protein alone was distributed diffusely throughout both the cytoplasm and the nucleus. To see if HA-tagged  $\lambda$  or  $\Delta$ K282W displayed the same subcellular localization as their GFP counterparts, HEK293 cells were cotransfected with GFP- $\lambda$  and HA- $\Delta$ K282W or GFP- $\Delta$ K282W and HA- $\Delta$ . The subcellular localization of HA- $\lambda$  and HA- $\Delta$ K282W was determined in fixed cells by immunocytochemistry using an anti-HA monoclonal antibody. As shown in Fig. 2B, HA- $\lambda$  was localized predominantly to the cytoplasm, whereas HA- $\Delta$ K282W accumulated in the nucleus. The nuclear localization of GFP- $\Delta$ K282W was also verified by confocal laser microscopy of transiently transfected NIH 3T3 cells (data not shown). Western blot analyses of whole cell extracts and immunostaining with a monoclonal antibody recognizing specifically the C-terminal catalytic domain of  $\lambda$ PKC showed that the nuclear staining was due to full-length protein and not caused by a proteolytic fragment containing GFP and only part of  $\lambda$ PKC (data not shown).

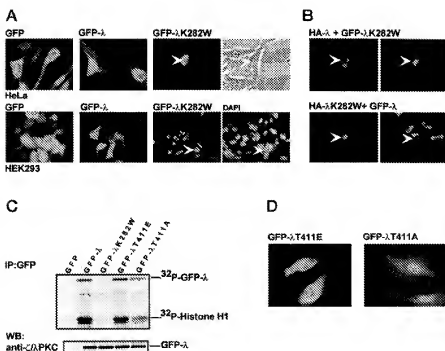
Phosphorylation of a conserved threonine residue within the activation loop of all PKCs is crucial for subsequent autophosphorylation and activation of the enzyme (54). Substitution of this threonine in  $\lambda$ PKC (Thr-410) with an acidic amino acid created a constitutively activated kinase, whereas replacing it with alanine severely reduced the catalytic activity (13, 55). To test if mutation of the corresponding Thr-411 site in  $\Delta$ PKC affected the subcellular localization of the kinase, GFP fusion proteins containing alanine (GFP- $\Delta$ T411A) or glutamate (GFP- $\Delta$ T411E) substitutions at this site were expressed in HeLa cells. The catalytic activity of the T411A mutant was significantly reduced compared with wild-type  $\lambda$ PKC and the T411E mutant (Fig. 2C). Interestingly, similar to the kinase-defective ATP-binding site mutant, GFP- $\Delta$ T411A was mainly nuclear in living HeLa cells, whereas GFP- $\Delta$ T411E displayed a predominantly cytosolic localization just as the wild-type  $\lambda$ PKC (Fig. 2D). Taken together, these results indicate that the ATP-binding site and the T411A mutations may somehow affect the overall conformation of the protein so that signals governing subcellular localization are exposed differently in these mu-

nants compared with the wild-type enzyme. However, as demonstrated below the observed nuclear accumulation is not correlated to the activity status of the kinase.

**The Zinc Finger Domain of  $\lambda$ PKC Contains a Nuclear Localization Signal.**—Proteins larger than about 40–60 kDa cannot enter into the nucleus through the nuclear pore complex by passive diffusion (38, 39). Since both HA- $\Delta$ K282W (67 kDa) and GFP- $\Delta$ K282W (92 kDa) are too large to diffuse into the nucleus, it seemed logical to assume that  $\lambda$ PKC could contain a functional nuclear localization signal (NLS) or be transported via interaction with a partner protein containing an NLS. Thus, to map the region(s) of  $\lambda$ PKC required for nuclear localization, deletion mutants were made in the context of GFP fusion proteins (Fig. 3A). Plasmids expressing the different deletions were transfected into HeLa cells, and the expression of GFP fusion proteins with correct sizes was verified by Western blot analyses using an anti-GFP antibody (Fig. 3B). Fluorescence microscopy of living cells revealed that GFP- $\Delta$ (256–595) corresponding to the catalytic domain of  $\lambda$ PKC was mainly localized diffusely in the cytoplasm (Fig. 3C). Due to a low level of expression of this construct in HeLa cells, GFP- $\Delta$ (256–595) was also transiently expressed in HEK293 cells. Compared with the distribution in HeLa cells, GFP- $\Delta$ (256–595) was even more excluded from the nucleus in HEK293 cells. In contrast, a fusion protein containing the regulatory domain, GFP- $\lambda$ (1–256) was primarily localized to the cell nucleus. We next analyzed which part of the regulatory domain that was responsible for the observed nuclear accumulation (Fig. 3C). GFP- $\lambda$ (1–139), containing the first 139 amino acids of  $\lambda$ PKC including the pseudosubstrate sequence, was diffusely localized throughout the cell. The molecular mass of this construct is ~42 kDa so the protein will probably enter the nucleus by passive diffusion (38, 39). In contrast, a GFP fusion protein corresponding to the zinc finger domain of  $\lambda$ PKC, GFP- $\lambda$ (141–194), was exclusively localized to the nucleus. This fusion protein further accumulated in structures corresponding to the nucleoli. These observations clearly suggest that the zinc finger domain contains a functional NLS. Surprisingly, GFP- $\lambda$ (194–256), containing the variable linker region between the zinc finger domain and the ATP-binding site, was excluded from the nucleus. According to the theoretical size of this fusion protein (about 35 kDa) one would expect that it could enter the nucleus by diffusion. Therefore, this fusion protein may be sequestered in the cytoplasm by an anchoring protein, or it may be actively exported from the nucleus.

The sequence identities between the zinc finger domain of  $\lambda$ PKC and those of classical and novel PKCs vary from 35 to 48%, whereas there is 74% identity between the zinc finger domains of  $\lambda$ PKC and  $\zeta$ PKC (Fig. 4A). We therefore asked whether the zinc finger domain of  $\zeta$ PKC, like that of  $\lambda$ PKC, was able to direct a GFP fusion protein to the nucleus. To this end, HeLa cells were transfected with a construct expressing a GFP fusion protein containing the complete zinc finger domain of murine  $\zeta$ PKC, GFP- $\zeta$ (130–182). Indistinguishable from the results with the corresponding  $\lambda$ PKC construct, this fusion protein was exclusively nuclear demonstrating that the zinc finger domain of  $\zeta$ PKC also contains an NLS (Fig. 4C). However, GFP fusion proteins containing either the first or both zinc finger domains of the classical isoform  $\alpha$ PKC, GFP- $\alpha$ (37–88), and GFP- $\alpha$ (37–155) did not accumulate in the cell nuclei but rather in punctate structures in the cytoplasm (Fig. 4C). Thus, the ability to translocate to the nucleus is not a conserved feature of PKC zinc finger domains.

The zinc finger domain of the  $\alpha$ PKCs does not contain classical monopartite or bipartite NLSs. However,  $\alpha$ PKC,  $\zeta$ PKC, and PKC $\delta$  from *Caenorhabditis elegans* contain a cluster of



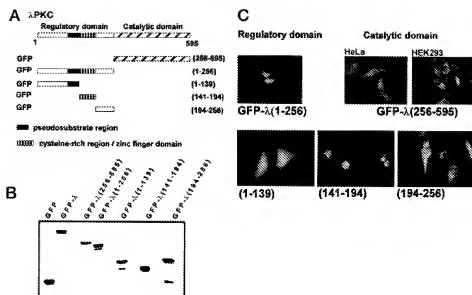
**Fig. 2. Different subcellular localization of wild-type APKC and two mutants with no or reduced activity.** *A*, subcellular distribution of GFP- $\Delta$  and kinase-defective GFP- $\Delta$ K282W in HeLa and HEK293 cells. Subconfluent cultures of HeLa (upper panel) or HEK293 (lower panel) cells seeded in 6-well dishes were transfected with 1  $\mu$ g of vectors expressing either GFP alone, GFP- $\Delta$ , or GFP- $\Delta$ K282W. The subcellular localization in living cells was visualized by fluorescence microscopy. HEK293 cells expressing GFP- $\Delta$ K282W were stained with DAPI to visualize the nuclei. The nuclei of HeLa and HEK293 cells expressing GFP- $\Delta$ K282W are indicated by arrows. *B*, similar subcellular distribution of HA-tagged (red) and GFP-tagged versions of wild-type and kinase-defective APKC. HEK293 cells were seeded in 24-well dishes and cotransfected with expression vectors (0.4  $\mu$ g) for HA- $\Delta$ K282W and GFP- $\Delta$ K282W (upper panel) or HA- $\Delta$ K282W and GFP- $\Delta$  (lower panel). Twenty-four h after transfection the cells were fixed and stained with an anti-HA antibody and analyzed by fluorescent microscopy. Arrows indicate the nuclei of coexpressing cells. *C*, kinase activity of different GFP- $\Delta$  mutants. Whole cell extracts from transiently transfected HeLa cells expressing either GFP alone, GFP- $\Delta$ , GFP- $\Delta$ K282W, GFP- $\Delta$ T411E, or GFP- $\Delta$ T411A were subjected to immunoprecipitation (IP) using an anti-GFP antibody. The kinase activities were determined using histone H1 as substrate. Autophosphorylation of immunoprecipitated proteins are indicated (<sup>32</sup>P-GFP- $\Delta$ ). The loading of immunoprecipitated proteins was visualized by immunoblotting with an antibody cross-reacting with both  $\zeta$ - and  $\Delta$ PKC. *D*, subcellular localization of GFP- $\Delta$ T411E and GFP- $\Delta$ T411A in transiently transfected HeLa cells.

four basic amino acids in the N-terminal part of the zinc finger (KRFLNRR in Fig. 4A). This motif is not found in the classical and novel PKCs as exemplified by the second zinc finger of  $\delta$ PKC and both zinc fingers of  $\alpha$ PKC in Fig. 4A. In a three-dimensional structure model of the zinc finger domain of APKC, constructed based on the solved structure of the corresponding zinc finger of  $\delta$ PKC, these basic residues are exposed on the surface. Particularly, Arg-150 and Arg-151 are ideally positioned to interact with either lipid cofactors or other proteins (Fig. 4B). To see if introduction of two acidic amino acids in this sequence could interfere with the nuclear localization of kinase-defective APKC, Arg-150 and Arg-151 were substituted with glutamate residues giving GFP- $\Delta$ K282W-R150E/R151E. Interestingly, these mutations abolished the nuclear accumulation of kinase-defective GFP- $\Delta$ K282W. GFP- $\Delta$ K282W-R150E/R151E was either diffusely distributed throughout the cells or totally excluded from the nucleus (Fig. 4D). Thus, Arg-150 and Arg-151 seem to be critically involved in nuclear localization of APKC. To see if the N-terminal half of the APKC zinc finger, including the critical arginine residues, was sufficient for mediating nuclear translocation, GFP- $\Delta$ (141–162) encoding a GFP fusion protein containing the first 22 amino acids of the zinc finger was made. GFP- $\Delta$ (141–162) accumulated in the nuclei of transiently transfected HeLa cells (Fig. 4E). In contrast to the GFP fusion protein containing the complete zinc finger, GFP- $\Delta$ (141–162) did not accumulate in the nuclei. Next, we mutated Arg-150 and Arg-151 in the context of the GFP- $\Delta$ (141–162) protein. GFP- $\Delta$ (141–162)R150E/R151E displayed the same diffuse subcellular distribution as GFP itself (Fig. 4E). Thus, our results strongly suggest that APKC contains a func-

tional NLS within the first 22 amino acids of the zinc finger domain and that Arg-150 and Arg-151 are critical residues within this NLS.

**Leptomycin B Treatment Induces Nuclear Accumulation of APKC**—To determine whether the predominantly cytoplasmic localization of wild-type APKC is caused by the presence of a leucine-rich NES, GFP- $\Delta$ -transfected HeLa cells were treated with leptomycin B (LMB). Interestingly, treatment with LMB for 2 h induced nuclear accumulation of the fusion protein (Fig. 5A). To determine whether LMB could induce nuclear accumulation of endogenous APKC, HeLa cells were either left untreated or treated with LMB for 2 h. The cells were fixed and the subcellular localization of endogenous APKC was determined by immunocytochemistry using a specific anti-APKC antibody. In untreated cells APKC was diffusely localized mainly in the cytoplasm with only a fraction of the protein in the nucleus (Fig. 5B, left panel). Importantly, LMB treatment induced redistribution of endogenous APKC from the cytoplasm to the nucleus (Fig. 5B, right panel). The nuclear accumulation of endogenous APKC in response to LMB was rapid, being significant after 15 min and almost completed after 30 min (Fig. 5C). These results demonstrate that APKC is exported from the nucleus by a mechanism either involving a functional *cis*-acting, LMB-sensitive NES or via an NES-containing interaction partner.

**Characterization of an NES within APKC**—Since GFP- $\Delta$ (194–256), despite of its small size, was completely excluded from the nucleus (see Fig. 3C), we speculated that this part of APKC, corresponding to the linker region between the zinc finger domain and the ATP-binding site, could be involved in



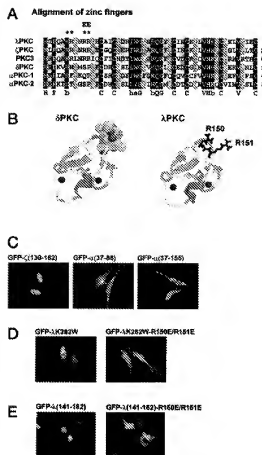
**Fig. 3. Expression and subcellular localization of GFP fusion proteins containing different parts of the  $\lambda$ PKC protein.** *A*, schematic representation of different GFP- $\lambda$  constructs. The numbers in parentheses refer to amino acid positions defining the parts of the  $\lambda$ PKC protein included in the fusions. *B*, immunoblotting of GFP- $\lambda$  deletion mutants. HEK293 cells were transfected with either pGFP-C1 or 10  $\mu$ g of expression vectors for other GFP- $\lambda$  constructs, GFP- $\lambda$ (256–595), GFP- $\lambda$ (1–139), GFP- $\lambda$ (141–194), or GFP- $\lambda$ (194–256). The cells were harvested 24 h post-transfection, and total cellular proteins were separated in 10% SDS-polyacrylamide gels. The proteins were electrotransferred to a membrane that was subsequently probed with an anti-GFP antibody. *C*, subcellular localization of the indicated GFP- $\lambda$  deletion mutants.

active export from the nucleus. Interestingly, we identified a region (amino acids 248–255) that displayed significant similarity to previously identified NES sequences (Fig. 6A). To determine whether this region mediates nuclear export of  $\lambda$ PKC, we generated a mutant of  $\lambda$ PKC in which two presumably critical hydrophobic amino acids, Phe-253 and Leu-255, are replaced by alanine residues. Similar mutations within NES sequences in other proteins abolish the function of the NES (41–43, 45, 46). In contrast to the wild-type kinase, GFP- $\lambda$ F253A/L255A accumulated in the nucleus (Fig. 6B). This strongly suggests that cytoplasmic localization of  $\lambda$ PKC is conferred by an NES in the linker region between the regulatory and the catalytic domains.

**Intramolecular Interactions between the N-terminal Pseudosubstrate Sequence and the Catalytic Domain Inhibit Nuclear Localization of  $\lambda$ PKC.**—To begin unraveling whether intramolecular interactions between the N-terminal part and the catalytic domain might mask the NLS in  $\lambda$ PKC, a GFP- $\lambda$  fusion protein in which the first 140 amino acids were deleted was transiently expressed in HeLa cells. Contrary to the full-length, wild-type kinase, GFP- $\lambda$ (141–595) localized exclusively to the nucleus (Fig. 7). Since this fusion protein lacks the autoinhibitory pseudosubstrate sequence, the kinase activity of GFP- $\lambda$ (141–595) was increased compared with the wild-type enzymes (data not shown). To determine whether disruption of the intramolecular interaction between the pseudosubstrate sequence and the catalytic domain led to nuclear localization, a point mutant of GFP- $\lambda$  in which Ala-129 within the pseudosubstrate sequence was replaced by glutamate, GFP- $\lambda$ A129E, was generated and transiently expressed in HeLa cells. Such a mutant has previously been demonstrated to be constitutively activated presumably due to the lack of interaction of the pseudosubstrate sequence with the substrate interaction site in the catalytic domain (56). Consistent with the notion of a conformational change exposing the NLS, GFP- $\lambda$ A129E displayed nuclear accumulation (Fig. 7). Taken together, these results and those presented earlier indicate that it is not the activity status of the kinase as such that determines the subcellular localization. Instead, intramolecular interactions between the catalytic domain and the pseudosubstrate sequence inhibit the

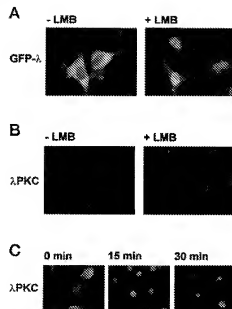
nuclear localization of  $\lambda$ PKC by inducing a conformation where the NLS is masked.

**Nuclear Import of  $\zeta$ PKC Is Much Less Efficient Than That of  $\lambda$ PKC in LMB-treated HeLa Cells.**—The  $\lambda$ PKC subtypes,  $\lambda$ PKC and  $\zeta$ PKC, have the same structural organization and display considerable sequence homology especially within their catalytic domains. To establish if  $\zeta$ PKC was similarly distributed within the cell as  $\lambda$ PKC, we made a vector expressing GFP fused to full-length  $\zeta$ PKC, pGFP- $\zeta$ . GFP- $\zeta$  was exclusively localized to the cytoplasm in untreated cells. Surprisingly, GFP- $\zeta$  did not accumulate in the nucleus upon LMB treatment for 2 h but was distributed diffusely all over the cell (Fig. 8A). However, after long term treatment with LMB (16 h), GFP- $\zeta$  accumulated in the nuclei of the transfected cells (data not shown). Since we did not have antibodies available that will only recognize  $\zeta$ PKC specifically, without detecting  $\lambda$ PKC, we were not able to analyze the subcellular distribution of endogenous  $\zeta$ PKC by immunocytochemistry. To test whether kinase-defective  $\zeta$ PKC localized differently from wild-type  $\zeta$ PKC, GFP- $\zeta$ K281W mutated in the ATP-binding site was expressed in HeLa cells. Contrary to kinase-defective  $\lambda$ PKC, GFP- $\zeta$ K281W was predominantly localized in the cytoplasm in a manner similar to wild-type GFP- $\zeta$  (Fig. 8C). Kinase assays performed following immunoprecipitation of GFP- $\zeta$  or GFP- $\zeta$ K281W from extracts of transiently transfected HeLa cells showed that GFP- $\zeta$  was active, whereas GFP- $\zeta$ K281W had no intrinsic kinase activity (Fig. 8C). Similar to GFP- $\lambda$ , GFP- $\zeta$  was as active as an HA epitope-tagged  $\zeta$ PKC (data not shown). Next, we mutated the putative NES sequence in GFP- $\zeta$  generating GFP- $\zeta$ F252A/L254A. Compared with wild-type GFP- $\zeta$ , this construct distributed more diffusely all over the cells in transiently transfected HeLa cells but in contrast to GFP- $\lambda$ F253A/L255A, GFP- $\zeta$ F252A/L254A did not accumulate in the nucleus (data not shown). Taken together these results indicate that the nuclear import of  $\zeta$ PKC is much less efficient than that of  $\lambda$ PKC. To sort out if this is due to intrinsic differences in the relative strength/exposure of the NLS and NES in the two kinases, several GFP- $\zeta$  deletion mutants were made, and their subcellular distribution was compared with the distribution of corresponding GFP- $\lambda$  mutants. Very interestingly, GFP- $\zeta$ L30–

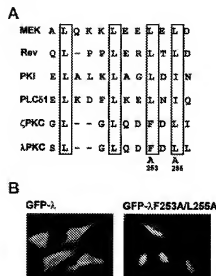


**Fig. 4. The zinc finger region of atypical PKCs contain a nuclear localization signal.** *A*, alignments of amino acid sequences of the zinc finger domains of murine  $\lambda$ PKC (SwissProt accession number Q62074), rat  $\zeta$ PKC (P09217), PKC $\delta$  from *C. elegans* (GenBank accession number AF025666), murine  $\delta$ PKC (P28867), and murine  $\alpha$ PKC (P20441). The sequences of both zinc finger domains of  $\alpha$ PKC are shown with  $\lambda$ PKC-1 as the most N-terminal zinc finger. Asterisks above the alignment denote the basic residues in the putative core NLS. The location of the two Arg residues mutated to Glu is indicated (*EE*). Conserved positions are indicated below the alignment (*b*, basic; *h*, hydrophobic; and *a*, aromatic). *B*, a three-dimensional structure model of the zinc finger domain of murine  $\lambda$ PKC is shown to the right with the Arg-150 and Arg-151 residues indicated. The side chains of other Arg and Lys residues are also shown (*blue*). The model was obtained from the Swiss Model Repository. The x-ray structure model of the second zinc finger of  $\delta$ PKC with the phorbol ester 12-*O*-tetradecanoylphorbol-13-acetate (in space-filling mode) bound and the two zinc atoms is shown to the left (*77*). *C*, subcellular localization of GFP fusions containing zinc finger regions of  $\zeta$ PKC and  $\lambda$ PKC. Constructs encoding GFP- $\zeta$ (130–182) containing the zinc finger region of murine  $\zeta$ PKC, GFP- $\lambda$ (37–88) containing the first zinc finger of  $\lambda$ PKC, and GFP- $\lambda$ (37–155) containing both zinc fingers of  $\lambda$ PKC were expressed in HeLa cells. *D*, mutation of Arg-150 and Arg-151 within the zinc finger of  $\lambda$ PKC prevents nuclear accumulation of kinase-defective  $\lambda$ PKC. The subcellular localization of GFP- $\lambda$ K282W and GFP- $\lambda$ K282W-R150E/R151E in which Arg-150 and Arg-151 are replaced by glutamine residues was analyzed in HeLa cells. *E*, GFP- $\lambda$ (141–162) containing the first 22 amino acids of the  $\lambda$ PKC zinc finger accumulates in the nucleus, whereas the NLS mutant GFP- $\lambda$ (141–162)-R150E/R151E is diffusely localized throughout the cell.

592) that lacks the first 129 amino acids of  $\zeta$ PKC, including the pseudosubstrate sequence, displayed the complete opposite localization compared with the corresponding GFP- $\lambda$ (141–595) being entirely excluded from the nucleus (Fig. 8D). However, LMB treatment induced rapid nuclear accumulation of this construct. Fig. 9 gives an overview of the subcellular localization of various GFP- $\lambda$  and  $\zeta$ -mutants before and after LMB treatment. Our observations indicate that in  $\zeta$ PKC the NES is a stronger signal than the NLS, and nuclear localization is only



**Fig. 5. LMB induces nuclear accumulation of GFP- $\lambda$  and endogenous  $\lambda$ PKC.** *A*, HeLa cells were transfected with expression vector for GFP- $\lambda$  as described in the legend to Fig. 3A. Twenty four h after transfection, cells were either left untreated or treated with 2  $\mu$ g/ml LMB for 2 h, and the subcellular localization of GFP- $\lambda$  was determined. *B*, HeLa cells were cultured in Eagle's minimum essential medium supplemented with 10% fetal calf serum and either left untreated or treated with LMB (2  $\mu$ g/ml) for 2 h. The cells were fixed, permeabilized, and stained with an anti- $\lambda$ PKC antibody that shows no cross-reactivity against  $\zeta$ PKC. *C*, an experiment performed similarly as in *B* except that LMB treatment was for 0-, 15- and 30 min, respectively.



**Fig. 6. Characterization of an NES within the linker region of APKC.** *A*, alignments of NES sequences from mitogen-activated protein kinase/extracellular signal-regulated kinase (439), PKI (42), Rev (41/18), PLC $\delta$ 1 (46), and the atypical PKCs. Important hydrophobic residues are boxed. *B*, mutation of critical hydrophobic residues within the NES (Phe-253 and Leu-255) blocks nuclear export of  $\lambda$ PKC. HeLa cells were transiently transfected with expression vectors for GFP- $\lambda$  or for GFP- $\lambda$ F253A/L255A, and the subcellular localization was determined 24 h after transfection.

observed when the NES motif is removed or functionally inhibited. In contrast, in  $\lambda$ PKC the NLS is more potent than the NES when both signals are exposed, and the nuclear import of  $\lambda$ PKC is much more efficient than that of  $\zeta$ PKC.

#### DISCUSSION

Nuclear localization of classical and novel PKCs as well as  $\alpha$ PKCs has been observed previously (8, 35, 58–64). However,



Fig. 7. Intramolecular interactions between the N-terminal pseudosubstrate sequence and the catalytic domain inhibit nuclear localization of  $\lambda$ PKC. HeLa cells were transfected with the indicated GFP- $\lambda$  fusion constructs, and the subcellular localization was determined 24 h following transfection.

to our knowledge, this is the first report where functional NLS and NES sequences are identified within any PKC. We find that  $\lambda$ PKC shuttles very rapidly and continuously between the nucleus and the cytoplasm. This rapid nucleocytoplasmic shuttling occurs both in noncycling serum-starved cells and in cycling cells proliferating in serum.

Our results suggest that the core of the NLS of  $\lambda$ PKC consists of the hexapeptide KRFNRR located in the N-terminal part of the zinc finger domain (amino acids 146–151). This basic cluster is conserved in  $\alpha$ PKCs from different species as well as in *C. elegans* PKC3 (KRLNRR) but not in classical and novel PKCs (Fig. 4A). An exception is provided by murine  $\epsilon$ PKC which contains a Gly residue instead of an Arg (KRFNRR), whereas the rat sequence contains the Arg. GFP fusion proteins containing the zinc finger region of either  $\lambda$ PKC or  $\epsilon$ PKC (both rat and murine) localize exclusively to the nucleus. In contrast, GFP fusion constructs expressing either one or both zinc fingers of classical  $\alpha$ PKC are excluded from the nucleus and rather distributed into punctate structures in the cytoplasm. A recent report (65) demonstrated that GFP fusion constructs that expressed only one or both of the zinc fingers of  $\gamma$ PKC localized to the cytoplasm of rat basophilic leukemia cells. Upon treatment with various stimuli including phorbol esters, the zinc finger region of  $\gamma$ PKC translocated to the plasma membrane. Thus, although evident for the  $\alpha$ PKCs, nuclear localization is not a conserved feature of PKC zinc fingers as such.

Based on sequence analyses it has been suggested that both the classical and the  $\alpha$ PKCs may contain a bipartite NLS (35). For  $\lambda$ PKC this NLS would encompass two basic amino acids in the pseudosubstrate sequence (Arg-133 and Lys-134) and Arg-150 and Arg-151 in the motif identified by us (KRFNRR) in the zinc finger domain. Two such basic clusters within a bipartite NLS are interdependent on each other to mediate nuclear localization (36). The GFP construct containing the zinc finger region lacks the upstream basic cluster in this suggested bipartite NLS. Since this construct is exclusively localized to the cell nucleus, we do not think that a bipartite NLS is involved in nuclear translocation of  $\lambda$ PKC. The KRFNRR motif, although shorter, is most similar to a type of monopartite NLSs enriched in arginine residues identified in the Tat and Rev proteins of human immunodeficiency virus-1 and the Rex protein of human T-cell leukemia virus type 1. These proteins have been demonstrated to be imported into the nucleus by importin  $\beta$  in an importin  $\alpha$ -independent manner (66, 67).

We have found that in contrast to wild-type  $\lambda$ PKC that mainly localized to the cytoplasm, two different point mutations in the catalytic domain led to nuclear accumulation of full-length  $\lambda$ PKC. Nuclear accumulation also occurred with deletion mutants lacking either the catalytic domain or the 140 N-terminal amino acids including the pseudosubstrate sequence. Importantly, the A129E point mutation in the pseudosubstrate sequence, which disrupts the interaction between this autoinhibitory sequence and the substrate interaction site in the catalytic domain, also led to nuclear accumula-

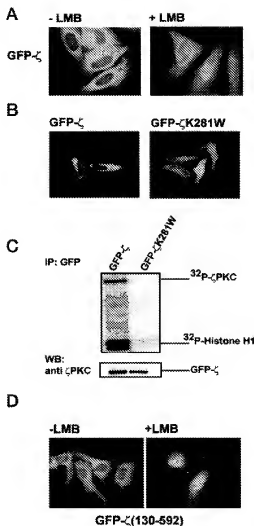


Fig. 8. GFP- $\zeta$  does not accumulate in the nucleus following a 2-h treatment with LMB. *A*, HeLa cells were seeded in 6-well dishes, and subconfluent cells were transfected with 1  $\mu$ g of a GFP construct containing wild-type rat  $\zeta$ PKC. Twenty-four h later the subcellular distribution of GFP- $\zeta$  was analyzed by fluorescence microscopy in cells which were either left untreated or treated with LMB (2 ng/ml) for 2 h. *B*, a kinase-defective mutant of  $\zeta$ PKC does not accumulate in the nucleus upon expression in HeLa cells. GFP- $\zeta$  and GFP- $\zeta$ K281W, which contain an inactivating mutation in the ATP-binding site, were expressed in HeLa cells. The subcellular localization was determined 24 h post-transfection. *C*, kinase activity of GFP- $\zeta$  and GFP- $\zeta$ K281W. HeLa cells were seeded in 100-mm dishes the day before transfection, and subconfluent cultures were transfected with 10  $\mu$ g of either an expression vector for GFP- $\zeta$  or an expression vector for GFP- $\zeta$ K281W. Cells were harvested 24 h after transfection, and the kinase activities of GFP- $\zeta$  and GFP- $\zeta$ K281W were assayed. Autophosphorylation of immunoprecipitated (IP) GFP- $\zeta$  is indicated. A Western blot (WB) of the immunoprecipitated proteins used in the kinase assays is also shown. *D*, deletion of the N-terminal regulatory domain containing the pseudosubstrate sequence of  $\zeta$ PKC does not cause nuclear accumulation in the absence of LMB (2 ng/ml for 2 h).

tion of full-length  $\lambda$ PKC fused to GFP. The deletion mutant is exclusively nuclear, whereas the point mutant is found also in the cytoplasm. This difference in the extent of relocalization relative to the wild-type enzyme is consistent with previous findings showing that regions of the regulatory domain of PKCs outside the pseudosubstrate sequence contribute to autoinhibition (68). We therefore suggest that intramolecular interactions between the catalytic domain and the N-terminal part of the protein regulate the conformation of the protein in such a way that the accessibility of the NLS, the NES, or both signaling sequences is affected. Such a model of regulation has been



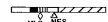

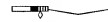

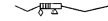

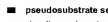
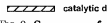
GFP- $\lambda$ - $\zeta$ fusion protein	$\lambda$ PKC		$\zeta$ PKC	
	- LMB	+ LMB	- LMB	+ LMB
	C	N	C	C(+N)
	N	C	C	C
	N		N	
	C+N	C+N	nd	nd
	N		C	N
	N		C+N	N
	N		N	
	C	N	nd	nd

Fig. 9. Summary of subcellular localizations of GFP fusion proteins containing full-length or different parts of  $\lambda$ - or  $\zeta$ PKC before and after LMB treatment. HeLa cells in 6-well dishes were transfected with 1  $\mu$ g of expression vector for each indicated GFP fusion protein and left untreated or treated with LMB (2  $\mu$ g/ml) for 2 h at 24 h post-transfection before being analyzed by fluorescence microscopy. The locations of the NLS and NES motifs are shown (open diamond and triangle, respectively). C, cytoplasm; N, nucleus; C+N, both cytoplasm and nucleus; nd, not determined.

suggested for the serine/threonine kinase MAPKAP kinase-2 (44). According to this model, an NLS within MAPKAP kinase-2 is exposed both in the inactive and active enzyme. In the inactive enzyme an NES motif is masked due to intramolecular interaction between an autoinhibitory region and the catalytic domain. Consequently, inactive MAPKAP kinase-2 is localized to the nucleus. However, upon phosphorylation and activation by p38, the intramolecular interaction is relieved leading to unmasking of the NES. When both the NLS and NES are exposed, the protein is exported from the nucleus more efficiently than it is imported (44). For  $\lambda$ PKC we suggest that it is primarily the exposure of the NLS that is regulated through intramolecular interactions between the catalytic domain and the N-terminal region. An interaction between the pseudosubstrate sequence in the N-terminal parts of the PKC enzymes and the substrate interaction site in the catalytic domain is well documented (69). To understand fully the intramolecular interactions regulating activity and subcellular localization, it will be necessary to determine the three-dimensional structure of both wild-type and mutant  $\lambda$ PKC.

As mentioned in the Introduction, nuclear localization of both  $\lambda$ PKC and  $\zeta$ PKC has been reported (8, 33, 35). Recently, it was shown that translocation of  $\zeta$ PKC to the nucleus following NGF stimulation of PC12 cells probably depends on nuclear PI 3-kinase activity (34). Interestingly, evidence for the existence of nuclear PI 3-kinase activity has been provided (70–72). It has earlier been proposed that conventional PKC isoforms may continuously shuttle in and out of the nucleus and become "trapped" in the nucleus by an increase in the nuclear level of diacylglycerol (73). In line with this hypothesis, Neri *et al.* (34) suggest that  $\zeta$ PKC is similarly trapped following an increase in nuclear phosphatidylinositol 3,4,5-trisphosphate. Due to their large size a functional NLS is required for nuclear import of  $\lambda$ PKCs. We find that the zinc finger domain contains a functional, although atypical, basic NLS. This signal functions independently of a structurally intact zinc finger in the context of a GFP fusion. However, we cannot rule out the possibility that in the context of the full-length protein an intact zinc finger is

required for nuclear accumulation. This is particularly the case since the two Arg residues we mutated to Glu resulting in loss of nuclear import may also be involved in the binding of phosphatidylinositol 3,4,5-trisphosphate. Thus, a conformational change may expose the NLS which then enables nuclear import. Subsequently, the protein may become trapped in the nucleus due to binding of nuclear phosphatidylinositol 3,4,5-trisphosphate by the zinc finger.

We find that  $\zeta$ PKC is much more inefficiently imported into the nucleus than  $\lambda$ PKC upon inhibition of nuclear export. This is in apparent conflict with the work showing rapid nuclear translocation of  $\zeta$ PKC following NGF treatment of PC12 cells. However, it is possible that nuclear translocation of  $\zeta$ PKC is more tightly regulated than that of  $\lambda$ PKC perhaps via post-translational modifications induced by specific stimuli. Another possibility is that both Neri *et al.* (34) and Wooten *et al.* (35) are actually looking more at  $\lambda$ PKC than  $\zeta$ PKC since the antibodies they used actually recognize both isoforms of  $\lambda$ PKCs. We find that PC12 cells express  $\lambda$ PKC using a specific monoclonal antibody recognizing only  $\lambda$ PKC. However, a similar antibody recognizing only  $\zeta$ PKC is not available.

In a recent study Sanchez *et al.* (57) reported that  $\lambda$ PKC colocalized with a putative anchoring protein called p62 into punctate, vesicle-like structures in the cytoplasm corresponding to late endosomes. The concept of p62 serving as an anchoring protein, or perhaps more precisely a scaffolding protein, for  $\lambda$ PKCs is very interesting since p62 also seems to be involved in recruiting other proteins into complexes harboring  $\lambda$ PKCs (74–76). We have found that, when overexpressed, p62 is able to redistribute kinase-defective  $\lambda$ PKC from the nucleus to the cytoplasm and that this ability is dependent on a direct interaction between these two proteins.<sup>2</sup> Thus, it is clear that in addition to regulation of subcellular localization by conformational changes affecting NLS and NES function, the localization of  $\lambda$ PKCs is also being regulated by proteins with scaffolding functions such as p62.

**Acknowledgments**—We are grateful to M. Yoshida for the generous gift of leptomycin B and to J. Moscat for pcDNA3-HA and pHA- $\zeta$ . We thank T. Larmark for helpful discussions.

#### REFERENCES

- Ron, D., and Kazanietz, M. G. (1999) *FASEB J.* **13**, 1658–1676
- Nishizuka, Y. (1995) *FASEB J.* **9**, 484–496
- Mellor, H., and Parker, P. J. (1998) *Biochem. J.* **332**, 281–292
- Ono, Y., Fujii, T., Ogita, K., Kikkawa, U., Igarashi, K., and Nishizuka, Y. (1989) *Proc. Natl. Acad. Sci. U.S.A.* **86**, 3099–3103
- Akimoto, K., Mizuno, K., Osada, S., Hirai, S., Tanuma, S., Suzuki, K., and Ohno, S. (1994) *J. Biol. Chem.* **269**, 12677–12683
- Muller, O., Ayoub, M., Storz, P., Renneke, J., Fabro, D., and Pfizenmaier, K. (1995) *EMBO J.* **14**, 1961–1969
- Lozano, J., Berra, E., Munio, M. M., Diaz-Meco, M. T., Dominguez, I., Sanz, L., and Moscat, J. (1994) *J. Biol. Chem.* **269**, 19200–19202
- Akimoto, K., Takahashi, R., Moriya, S., Nishio, N., Takayanagi, J., Kimura, K., Fukui, Y., Osada, S.-I., Mizuno, K., Hirai, S.-I., Kazanietz, A., and Ohno, S. (1996) *EMBO J.* **15**, 788–798
- Nakanishi, H., Browne, K. A., and Ertter, J. H. (1993) *J. Biol. Chem.* **268**, 13–16
- Standert, M. L., Galloway, L., Karnam, P., Bandopadhyay, G., Moscat, J., and Farsese, R. V. (1997) *J. Biol. Chem.* **272**, 30075–30082
- Sontag, E., Sontag, J. M., and Garcia, A. (1997) *EMBO J.* **16**, 5662–5671
- Herreros Valls, P., Kautson, K. L., and Reiter, N. E. (1997) *J. Biol. Chem.* **272**, 16445–16452
- Chou, M.-M., Hou, W., Johnson, J., Graham, L.-K., Lee, M.-H., Chen, C.-S., Newton, A. C., Schaffhausen, B. S., and Tokar, A. (1998) *Curr. Biol.* **8**, 1069–1077
- Takeda, H., Matsuzaki, T., Takeda, T., Naguchi, T., Yamao, T., Tsuda, M., Oishi, F., Fukunaga, K., Inagaki, K., and Kaanga, M. (1999) *EMBO J.* **18**, 386–395
- Dominguez, I., Diaz-Meco, M. T., Munio, M. M., Berra, E., Garcia de Herreros, A., Cornet, M. E., Sanz, L., and Moscat, J. (1992) *Mol. Cell. Biol.* **12**, 3778–3783
- Berra, E., Diaz-Meco, M. T., Dominguez, I., Munio, M. M., Sanz, L., Lozano, J., Chapkin, R. S., and Moscat, J. (1993) *Cell* **74**, 555–563
- Coleman, E. S., and Wooten, W. W. (1994) *J. Mol. Neurosci.* **5**, 39–57
- Wooten, W. W., Zhou, G., Seibenhener, M. L., and Coleman, E. S. (1994) *Cell*

<sup>2</sup> M. Perander, G. Björkoy, T. Larmark, and T. Johansen, manuscript in preparation.

- Growth Differ. 5, 395-403
19. Liu, Q., Ning, W., Dantzer, R., Freund, G. G., and Kelley, K. W. (1998) *J. Immunol.* **160**, 1393-1401
  20. Brazil, D. P., and Hemmings, B. (2000) *Curr. Biol.* **10**, 592-594
  21. Mendez, R., Kollmann, G., White, M. F., and Rhoads, R. E. (1997) *Mol. Cell Biol.* **17**, 5184-5192
  22. Bandyopadhyay, G., Standaert, M. L., Kikkawa, U., Ono, Y., Moscat, J., and Farese, R. V. (1999) *Biochem. J.* **337**, 461-470
  23. Standaert, M. L., Bandyopadhyay, G., Sulam, M. F., Cong, L., Quon, M. J., and Farese, R. V. (1999) *J. Biol. Chem.* **274**, 14074-14078
  24. Kotani, K., Ogawa, W., Matsumoto, M., Kitamura, T., Sakae, H., Hino, Y., Miyake, K., Sano, W., Akimoto, K., Ohno, S., and Kaasuga, M. (1998) *Mol. Cell Biol.* **18**, 6971-6982
  25. Xu, J., Zaitsev, M. M., Santoro, S. A., and Clark, R. A. (1996) *J. Cell Biol.* **134**, 1301-1311
  26. Diaz-Meco, M. T., Municio, M. M., Frutos, S., Sanchez, P., Lozano, J., Sanz, L., and Moscat, J. (1996) *Cell* **86**, 777-786
  27. Berra, E., Municio, M. M., Sanz, L., Frutos, S., Diaz-Meco, M. T., and Moscat, J. (1997) *Mol. Cell Biol.* **17**, 4346-4354
  28. Murray, N. R., and Fields, A. P. (1997) *J. Biol. Chem.* **272**, 27521-27524
  29. Diaz-Meco, M. T., Lalleu, M. J., Monjas, A., Frutos, S., and Moscat, J. (1999) *J. Biol. Chem.* **274**, 19606-19612
  30. Frutos, S., Moscat, J., and Diaz-Meco, M. T. (1999) *J. Biol. Chem.* **274**, 10765-10770
  31. Municio, M. M., Lazano, J., Sanchez, P., Moscat, J., and Diaz-Meco, M. T. (1995) *J. Biol. Chem.* **270**, 15884-15891
  32. Pal, S., Claffey, K. P., Cohen, H. T., and Mukhopadhyay, D. (1998) *J. Biol. Chem.* **273**, 29277-29280
  33. Zhou, G., Seibenhener, M. L., and Wooten, M. W. (1997) *J. Biol. Chem.* **272**, 31130-31137
  34. Neri, L. M., Martelli, A. M., Borgatti, P., Colomusi, M. L., Marchisio, M., and Capitani, S. (1999) *FASEB J.* **13**, 2299-2310
  35. Wooten, M. W., Zhou, G., Wooten, M. C., and Seibenhener, M. L. (1997) *J. Neurosci. Res.* **49**, 353-403
  36. Dingwall, C., and Laskey, R. A. (1991) *Trends Biochem. Sci.* **16**, 478-481
  37. Conti, E., Uy, M., Leighton, L., Blobel, G., and Kuriyan, J. (1998) *Cell* **94**, 129-204
  38. Gorlich, D. (1998) *EMBO J.* **17**, 2721-2727
  39. Nigg, E. A. (1997) *Nature* **386**, 779-787
  40. Adam, S. A. (1999) *Curr. Opin. Cell Biol.* **11**, 402-406
  41. Fischer, U., Huber, J., Boelen, W. C., Mattaj, J. W., and Luhrmann, R. (1995) *Cell* **82**, 475-483
  42. Wen, W., Menikoff, J. L., Tsien, R. Y., and Taylor, S. S. (1995) *Cell* **82**, 463-473
  43. Fukuda, M., Gotoh, I., Gotoh, Y., and Nishida, E. (1998) *J. Biol. Chem.* **273**, 20024-20028
  44. Engel, K., Kolyarov, A., and Gaehtel, M. (1998) *EMBO J.* **17**, 3363-3371
  45. Toyoshima, F., Moriguchi, T., Wada, A., Fukuda, M., and Nishida, E. (1998) *EMBO J.* **17**, 2728-2735
  46. Yamaga, M., Fujii, M., Kamata, H., Hirata, H., and Yagisawa, H. (1999) *J. Biol. Chem.* **274**, 28557-28561
  47. Fukuda, M., Asano, S., Nakamura, T., Adachi, M., Yoshida, M., Yanagida, M., and Nishida, E. (1997) *Nature* **390**, 308-311
  48. Fornerod, M., Ohno, M., Yoshida, M., and Mattaj, J. W. (1997) *Cell* **90**, 1051-1060
  49. Stade, K., Ford, C. S., Guthrie, C., and Weiss, K. (1997) *Cell* **90**, 1041-1050
  50. Osareh-Nazari, B., Bachelier, F., and Dargemont, C. (1997) *Science* **278**, 141-144
  51. Kudo, N., Matsumori, N., Teoka, H., Fujiwara, D., Schreiner, E. P., Wolff, B., Yoshida, M., and Horinouchi, S. (1999) *Proc. Natl. Acad. Sci. U. S. A.* **96**, 9112-9117
  52. Solbie, L. A., Schitz-Peffier, C., Sheng, Y., and Biden, T. J. (1993) *J. Biol. Chem.* **268**, 24936-24942
  53. Noss, M. A., Baglia, L. A., Antinore, M. J., Ludlow, J. W., and McCance, D. J. (1998) *EMBO J.* **17**, 2342-2352
  54. Orr, J. W., and Newton, A. C. (1994) *J. Biol. Chem.* **269**, 27715-27718
  55. Le Good, J. A., Ziegler, W. H., Parekh, D. B., Alessi, D. R., Cohen, P., and Parker, P. J. (1998) *Science* **281**, 2042-2045
  56. Uebachs, P., Gschlecht, S., Halber, K., Presser, P., Bauer, B., Gschwendt, M., Grunke, H. H., and Baier, G. (1997) *J. Biol. Chem.* **272**, 4072-4078
  57. Sanchez, P., De Carcer, C., Sandoval, I. V., Moscat, J., and Diaz-Meco, M. T. (1998) *Mol. Cell Biol.* **18**, 3089-3090
  58. Bastiani, P. L., and Jovin, T. M. (1996) *Proc. Natl. Acad. Sci. U. S. A.* **93**, 8407-8412
  59. Greif, H., Ben-Chaim, J., Shimon, T., Bechor, E., Eldar, H., and Livneh, E. (1992) *Mol. Cell Biol.* **12**, 1304-1311
  60. Hoevar, B. A., and Fields, A. P. (1991) *J. Biol. Chem.* **266**, 28-33
  61. James, G., and Olson, E. (1992) *J. Cell Biol.* **116**, 863-874
  62. Leach, K. L., Ruff, V. A., Jarpe, M. R., Adams, L. D., Fabbro, D., and Raben, D. M. (1992) *J. Biol. Chem.* **267**, 21816-21822
  63. Rosenberger, U., Shukla, M., and Buchner, K. (1995) *Biochem. J.* **305**, 269-275
  64. Schmalz, D., Hache, F., and Buchner, K. (1998) *J. Cell Sci.* **111**, 1829-1839
  65. Canessa, F., Turel, M. N., Quest, A. F., and Meyer, T. (1998) *J. Cell Biol.* **140**, 485-498
  66. Palmeri, D., and Malin, M. H. (1999) *Mol. Cell Biol.* **19**, 1218-1225
  67. Truett, R., and Cullen, B. R. (1999) *Mol. Cell Biol.* **19**, 1210-1217
  68. Parissenti, A. M., Kirwan, A. F., Kim, S. A., Colantonio, C. M., and Schimmer, R. P. (1998) *J. Biol. Chem.* **273**, 8940-8945
  69. Orr, J. W., and Newton, A. C. (1994) *J. Biol. Chem.* **269**, 8388-8397
  70. Metjian, A., Roll, R. L., Ma, A. D., and Abrams, C. S. (1999) *J. Biol. Chem.* **274**, 27943-27947
  71. Neri, L. M., Milani, D., Bertolotto, L., Strocchi, M., Bertagnolo, V., and Capitani, S. (1994) *Cell Mol. Biol.* **40**, 619-626
  72. Tanaka, K., Horiguchi, K., Yoshida, T., Takeda, M., Fujisawa, H., Takeuchi, K., Umeda, M., Kato, S., Ihara, S., Nagata, S., and Fukui, Y. (1999) *J. Biol. Chem.* **274**, 3919-3922
  73. Divecha, N., Banfil, H., and Irvine, R. F. (1993) *Cell* **74**, 405-407
  74. Gong, J., Xu, J., Bezanilla, M., van Huizen, R., Derin, R., and Li, M. (1999) *Science* **285**, 1565-1569
  75. Sanz, L., Sanchez, P., Lalleu, M. J., Diaz-Meco, M. T., and Moscat, J. (1999) *EMBO J.* **18**, 3044-3053
  76. Moscat, J., and Diaz-Meco, T. (2000) *EMBO Rep.* **1**, 399-403
  77. Zhang, G., Kazanietz, M. G., Blumberg, P. M., and Hurley, J. H. (1995) *Cell* **81**, 917-924